TẠP CHÍ KHOA HỌC
TRƯỜNG ĐẠI HỌC QUY NHƠN

Hoạt tính xúc tác quang phân hủy methylene blue bằng vật liệu nano bán dẫn ZnO pha tạp Eu và Mn: Một nghiên cứu so sánh

Nguyễn Thị Khả Vân[1], Imee Saladaga Padillo[2], Đinh Kha Lil[3,*]

[1]Trung tâm GDNN – GDTX quận Ninh Kiều, Việt Nam
[2]Khoa Công Nghệ, Đại học bang Eastern Visayas, Phi-líp-pin
[3]Khoa Khoa học Tự nhiên, Trường Đại học Cần Thơ, Việt Nam

Ngày nhận bài: 14/11/2022; Ngày sửa bài: 21/12/2022;
Ngày nhận đăng: 31/01/2023; Ngày xuất bản: 28/06/2023

TÓM TẮT

Nghiên cứu này được thực hiện nhằm tổng hợp vật liệu nano ZnO pha tạp Eu và Mn có tính chất quang học thích hợp cho ứng dụng quang xúc tác. Vật liệu nano ZnO với 1%, 5% và 10% mol kim loại pha tạp được điều chế bằng phương pháp thủy nhiệt. Các đặc tính cấu trúc, hình thái, quang học và từ tính của các hạt nano chuẩn bị được nghiên cứu bằng cách sử dụng nhiễu xạ tia X (X-ray diffraction - XRD), kính hiển vi điện tử quét (scanning electron microscope - SEM) và quang phổ phân tán năng lượng tia X (energy dispersion spectroscopy - EDS). Kết quả cho thấy các hạt nano ZnO pha tạp Eu và ZnO pha tạp Mn có cấu trúc wurtzite lục giác. Hoạt tính của các chất xúc tác quang đã tổng hợp được đánh giá dựa trên sự phân hủy quang của methylene blue (MB) dưới sự chiếu xạ tia UV. Vật liệu ZnO pha tạp 5% mol Eu và vật liệu ZnO pha tạp 1% mol Mn cho thấy hoạt tính quang xúc tác tốt nhất. Phản ứng phân hủy MB tuân theo quy luật động học của phản ứng bậc nhất. Vật liệu ZnO pha tạp kim loại tổng hợp rất dễ phục hồi và có khả năng tái sử dụng cao.

Từ khóa: *Tổng hợp ZnO cấu trúc nano, ZnO pha tạp kim loại, phương pháp thủy luyện, tính chất quang.*

**Tác giả liên hệ chính.*
Email: lildk93@gmail.com

QUY NHON UNIVERSITY
JOURNAL OF SCIENCE

Photocatalytic decomposition of methylene blue using Eu- and Mn-doped ZnO semiconductor nanomaterials: A comparative study

Kha-Van Nguyen-Thi[1], Padillo Imee Saladaga[2], Kha Lil Dinh[3,*]

[1]Center for Vocational Education - Secondary Education, Ninh Kieu District, Vietnam
[2]College of Engineering, Eastern Visayas State University, Philippines
[3]College of Natural Sciences, Can Tho University, Vietnam

Received: 14/11/2022; Revised: 21/12/2022;
Accepted: 31/01/2023; Published: 28/06/2023

ABSTRACT

This study was carried out to synthesize Eu- and Mn-doped ZnO nanomaterials with optical properties suitable for catalytic applications. ZnO nanomaterials with 1%, 5%, and 10% mol of dopant were prepared using hydrothermal method. The structural, morphological, optical, and magnetic properties of the as-prepared nanoparticles were investigated using X-ray diffraction (XRD), scanning electron microscope (SEM), and X-ray energy dispersion spectroscopy (EDS). The results showed that the Eu-doped ZnO and Mn-doped ZnO nanoparticles exhibited a hexagonal wurtzite structure. The activity of the prepared photocatalysts was evaluated based on the photodegradation of methylene blue (MB) under ultraviolet light UV. ZnO materials doped with 5% mol Eu and ZnO materials doped with 1% mol Mn showed the best photocatalytic activity. Furthermore, the MB photodegradation reaction was observed to follow a first-order reaction. Finally, synthesized metal-doped ZnO materials are easy to recover and highly reusable.

Keywords: *Synthesis ZnO nanostructures, Metal-doped ZnO, hydrothermal method, optical properties.*

1. INTRODUCTION

In recent years, surface water and groundwater pollution has increased due to population growth and industrial development.[1] The primary sources of environmental pollution are organic dyes used in the food and textile industries due to their high toxicity and non-biodegradability, which has a carcinogenic effect on humans.[2,3] Methylene blue (MB) dyes are used by various industries, for example, as dyes in silk; as a food additive; and as dyeing of wool, leather, cotton, jute, and paper.[4,5] Methylene blue dyes have potent effects on the immune and reproductive systems and have potential carcinogenic and genotoxic effects.[6,7] Therefore, these harmful dyes must be removed from industrial wastewater. Several methods, such as biological treatment,[8,9] adsorption,[10] and photocatalysis,[11,12] have been used to remove these dyes from industrial wastewater. The use of photocatalysts to reduce organic compounds or convert them into harmless chemicals has been extensively studied to reduce the damage caused by organic dye pollution to the environment and to humans.[13] Semiconductor oxides, such as TiO_2, ZnO,

**Corresponding author.*
Email: lildk93@gmail.com

https://doi.org/10.52111/qnjs.2023.17303

SnO_2, WO_2, and CeO_2, are abundant in nature and widely used as a photochemical catalysts, especially for heterogeneous processes.[14,15] Among them, ZnO oxide is considered to be a promising catalyst in the decomposition of organic pigments as well as water disinfection. The most significant advantage of ZnO over TiO_2 is that it absorbs a larger range of the ultraviolet (UV) spectrum and has a corresponding threshold of 425 nm. Upon illumination, valence band electrons are promoted to the conduction band leaving a hole behind. These electron–hole pairs can either recombine or interact separately with other molecules. The holes at the ZnO valence band can oxidize the adsorbed water molecules or hydroxide ions to produce hydroxyl radicals. Electrons in the conduction band on the catalyst surface can reduce molecular oxygen to superoxide anion. This radical may form organic peroxides or hydrogen peroxide in the presence of organic scavengers.[16] ZnO is also one of the dominant materials used for nanotechnology. With controlled and material-dependent properties such as chemical, structural, electrical, thermal, and surface properties that can be varied depending on shape size, it has a wide range of applications.[17-18] ZnO's structure, a sizeable band gap energy (3.37 eV), the large exciton binding energy (60 meV), size, and thermal stability make it suitable for a broader range of devices.[19,20] To expand the application scope of ZnO, it is necessary to change the nanostructures' electron properties, narrow the band gap energy, and reduce the rate of photogenerated electrons and holes recombination. Metal or nonmetal doping into ZnO network is one of the effective methods to increase the activity of ZnO,[21,22] In recent years, much effort has been made to prepare metal doped ZnO materials, and various methods such as sol–gel, micro-emulsion, hydrothermal, spray pyrolysis, solid-reaction, radio frequency reactive magnetron sputtering, and electrodeposition have been employed. It is reported that the surface defects, serving as energy traps, may play a key role in the process of energy transfer. Compared with other approaches, hydrothermal method is regarded as an attractive candidate for the synthesis of metal doped ZnO due to its simplicity, easy-control, low-cost, and especially the presence of a large amount of surface defects. In this paper, Mn- and Eu-doped ZnO nanopowders were prepared with different metal concentration (1, 5 and 10% wt.) using solid state reaction. The obtained product was investigated by various advanced analytical techniques. The obtained composite was tested for photocatalytic applications on in water under UV light.

2. MATERIALS AND METHODS

2.1. Nanostructures synthesis

The Mn- and Eu-doped ZnO photocatalysts were synthesized using the hydrothermal method. $ZnCl_2$ was dissolved in deionized water and stirred using a magnetic stirrer for 30 minutes. With constant stirring, the doped metal ion solution was added to the solution, and stirring was continued for 30 minutes. The mixture's pH was adjusted to pH = 10 using 1M NaOH, and the stirring was continued for one more hour. The entire mixture was transferred to a thermos Teflon flask and allowed to stabilize in the oven at 190°C for 20 hours. After the reaction time, the resulting solution was centrifuged at 5500 rpm, and the solids were washed three times with deionized water and three times with alcohol to separate them from the solution. The desired product was obtained after drying the solids at 100°C for 20 hours.

2.2. Characterization techniques

X-ray diffraction (XRD) measurements were obtained using a diffractometer X-ray on the Bruker D8 Advance device (Germany) with a wavelength of λ = 1.5406Å. The extension of the diffraction test peak can provide information about the average crystal size through Scherrer's equation (1):[23]

$$D = \frac{0,9\lambda}{\Delta(2\theta)\cos\theta} \quad (1)$$

Where D is the average crystal size and Δ(2θ) is the full width at half maximum (FWHM).

The metal distribution in the materials was characterized using a scanning electron microscope field emission scanning (SEM, Hitachi X650) equipped with an energy dispersion X-ray system (EDS).

2.3. Photocatalysis experiments

The photocatalytic activities of synthetic materials were assessed based on the photo-catalytic degradation reaction of MB. The remaining MB concentration over time of the photocatalytic reaction was determined on the UV-VIS Spectrophotometer Optima SP-3000 (Japan). A 20 W UV lamp was used as the light source for the photochemical reaction.

2.3.1. Establishment of a standard curve to investigate the linear range of the MB solution

MB solutions with a concentration of 100 mg/L were prepared and then diluted into the corresponding concentrations: 0.1, 0.5, 1.0, 1.5, 2.0, 4.0, 6.0, 8.0, 10.0, 12.0, 14.0, 16.0, 18.0, 20.0, 22.0, and 24.0 mg/L. UV-VIS spectroscopy was conducted with wavelengths ranging from 200 to 800 nm. Finally, the maximum absorption wavelength and linear range were determined, and the standard line of the MB solution was plotted.

2.3.2. Photocatalytic experiments

The adsorption of the dye to the surface of the catalyst is well known depending on the pH of the solution used.[24] Faouzi Achouri et al. showed that the catalytic activity was high for the doped ZnO materials at pH = 9.[25] A certain amount of synthetic material was added to 100 mL of the MB solution of pre-determined concentration, and then the pH was adjusted to pH = 9 using a 1M NaOH solution. The reaction mixture was stirred in the dark using a magnetic stirrer until the adsorption equilibrium was reached. 5 mL of the reaction mixture was centrifuged to separate the solids, and the optical density was measured (time t = 0, optical density A_o). Then the solution was stirred constantly and irradiated using a 20W UV bulb placed about 20 cm from the solution's surface. Every 30 minutes, 5 mL of the sample solution was taken and centrifuged to obtain the catalytic powder, and the optical density (A_t) was measured. This investigation was carried out for 270 minutes.

The decomposition efficiency of MB was calculated using equation (2):

$$H = \frac{C_o - C_t}{C_o} \times 100 = \frac{A_o - A_t}{A_o} \times 100 \qquad (2)$$

Where C_o is the initial concentration of MB and C_t is the concentration of MB at different irradiation times.

3. RESULTS AND DISCUSSION

3.1. The Eu-doped ZnO characteristics

3.1.1. Effect of the amount of Eu dopant

The XRD results (Figure 1a) show that the high-intensity diffraction peaks correspond to the network plane families (100), (002), (101), and diffraction peaks with lower intensity, respectively. Lattice plane (102), (110), (103), (200), (112), (201), this result is consistent with JCPDS Card No. 77-0452 of the characteristic of the ZnO lattice has a Wurtzite hexagonal structure.[26] The position of the (100) peak was slightly shifted toward the lower angles, indicating the substitution of Eu^{3+} in the ZnO lattice (Figure 1b).[27] As shown, the weakness of their full width at half maximum may indicate an improvement in the crystallinity of ZnO. Thus, the peak is shifted towards the lower angle side.[28]

Figure 1a shows that when the molar ratio of doped Eu is less than 5%, the resulting XRD pattern has a monophasic hexagonal ZnO structure. However, when the molar ratio of Eu is doped more than 5%, in addition to the hexagonal phase of ZnO, there is also a cubic Eu_2O_3 phase corresponding to the JCPDS Card No. 43-1008 tag of Eu_2O_3. The formation of the Eu_2O_3 phase when increasing the content of doped Eu can be explained because zinc ions and Eu ions have different charges, and their difference in radius is quite large (Eu^{3+}: 0.95 Å; Zn^{2+}: 0.74 Å).[29]

https://doi.org/10.52111/qnjs.2023.17303

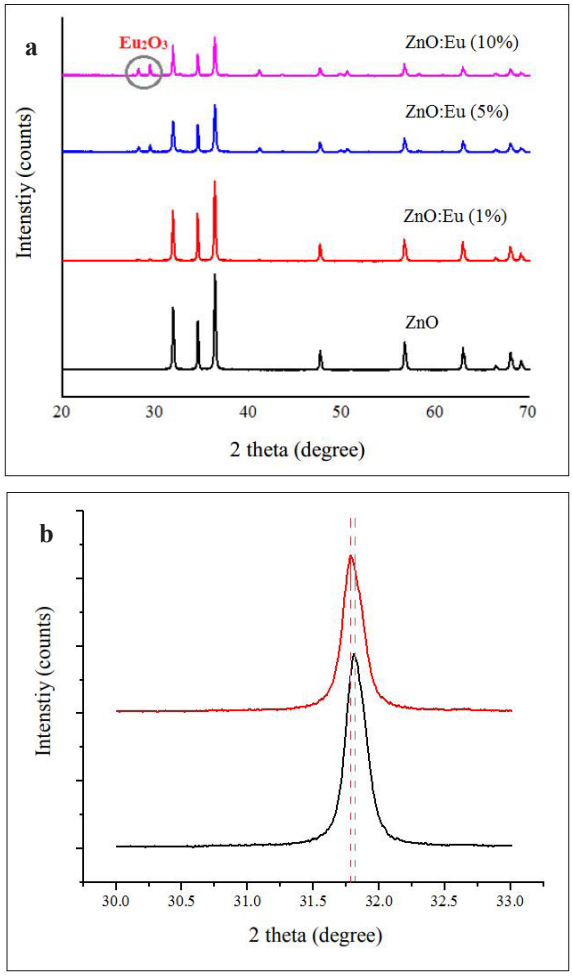

Figure 1. (a) The XRD patterns for Eu-doped ZnO with different doped Eu molar ratios; **(b)** Comparison of XRD diffraction peak positions of Eu-doped ZnO (red) and undoped ZnO (black).

Table 1. The crystal size of ZnO nanoparticles according to Eu^{3+} dopant concentration.

The concentration of doped Eu^{3+}	Δ (2θ) (radian)	2θ (degree)	D (nm)
1%	0.217	36.287	38.60
5%	**0.239**	**36.305**	**34.92**
10%	0.219	36.294	38.17

Table 1 shows that the material Eu-doped ZnO synthesized with a 5% mol doped manganese content has the smallest crystal size. Therefore, the 5% mol Mn-doped ZnO was selected to examine the characteristic properties and photo-oxidation capabilities through the photo-catalytic reaction.

3.1.2. Characteristic properties of Eu-doped ZnO material

Figure 2 shows the presence of Eu in the Eu-doped ZnO material over the EDS spectrum. This result shows the presence of elements such as Zn, O, and Eu in the sample. In addition, there was no foreign element present. These data again demonstrate the existence of europium in high-purity samples and prepared materials.

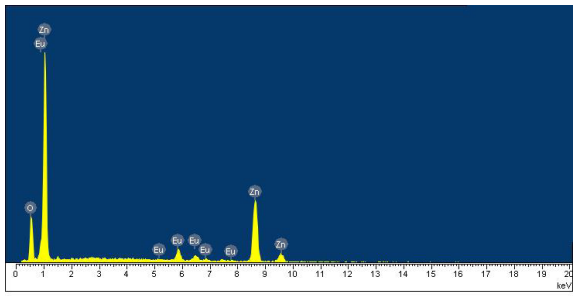

Figure 2. EDS spectra of (5%) Eu-doped ZnO nanoparticles.

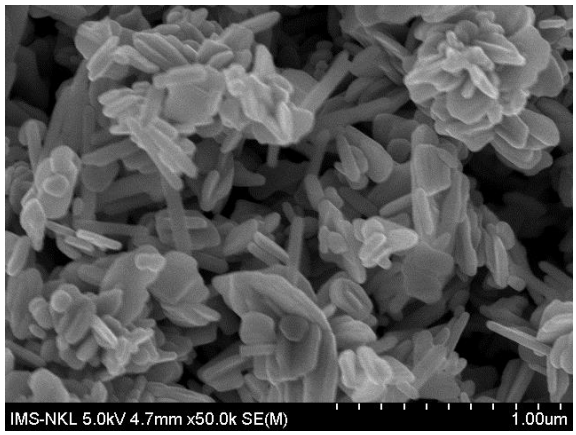

Figure 3. SEM images of (5%) Eu-doped ZnO nanoparticles.

The shape and size of Eu-doped ZnO are shown in the SEM image (Figure 3). The results of the SEM analysis show that Eu – ZnO particles are hexagonal in shape, with particle widths ranging from 32 to 72 nm and lengths from 127 nm to 367 nm.

3.2. The Mn-doped ZnO characteristics

3.2.1. Effect of the amount of Mn dopant

After synthesis, the Mn-doped ZnO materials were studied by using the XRD method. The results show that the concentration of Mn^{2+} ions does not affect the crystal phase composition.

No presence of diffraction peaks of manganese metal or manganese oxides was observed. Diffraction peaks correspond to the network plane families (100), (002), (101), (102), (110), (103) in accordance with the XRD scheme of the block ZnO - JCPDS Card No-00-036-145 (Figure 4). The XRD results also showed that the Mn^{2+} ions systematically replaced the Zn^{2+} ions in the sample without changing the wurtzite structure.[30]

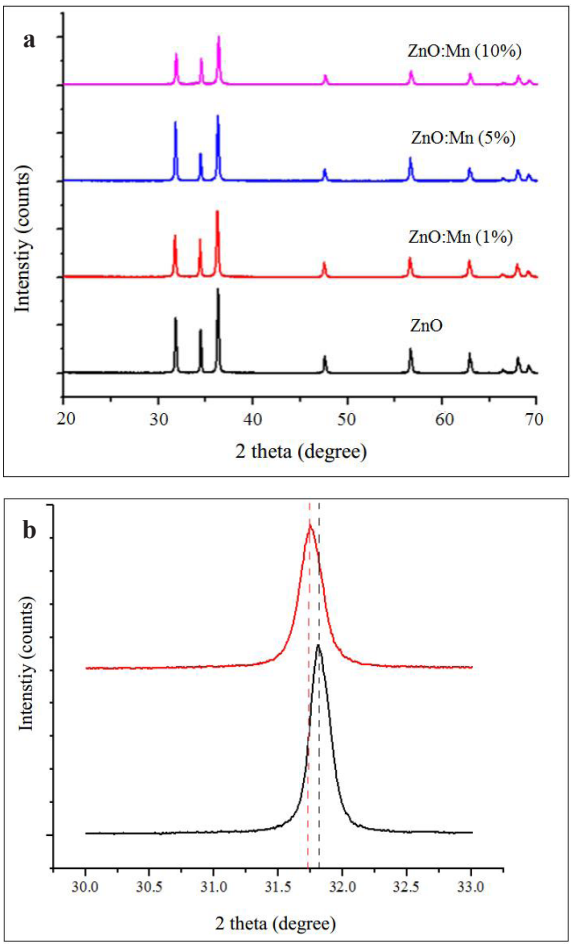

Figure 4. The XRD patterns for Mn-doped ZnO with different Mn dopant molar ratios, (b) Comparison of XRD diffraction peak positions of Mn-doped ZnO (red) and undoped ZnO (black).

The XRD results also show that the effect of the Mn dopant is related to the displacement of diffraction peaks towards a smaller 2 theta angle and a decrease in peak intensity compared to diffraction peaks of undoped ZnO. This fact (Figure 4a) shows that manganese was successfully doped into the ZnO network,[31] where the Mn^{2+} ions have replaced the Zn^{2+} ions. Mn^{2+} and Zn^{2+} ions have the same charge, and their ionic radius is not much different, so Mn^{2+} ions can easily enter the ZnO crystal lattice by partially replacing the Zn^{2+} ion's position or entering the lattice holes of ZnO.

Table 2 shows that the 1% (mol) Mn-doped ZnO material has the smallest crystal size. Therefore, the 1% mol Mn dopant concentration was chosen to examine its characteristic properties and photocatalytic.

Table 2. Effect of Mn doping on structural parameters of ZnO.

The concentration of doped Mn^{2+}	Δ (2θ) (radian)	2θ (degree)	D (nm)
1%	**0.222**	**36.240**	**37.65**
5%	0.205	36.291	40.78
10%	0.218	36.368	38.36

3.2.2. Characteristic properties of Mn-doped ZnO material

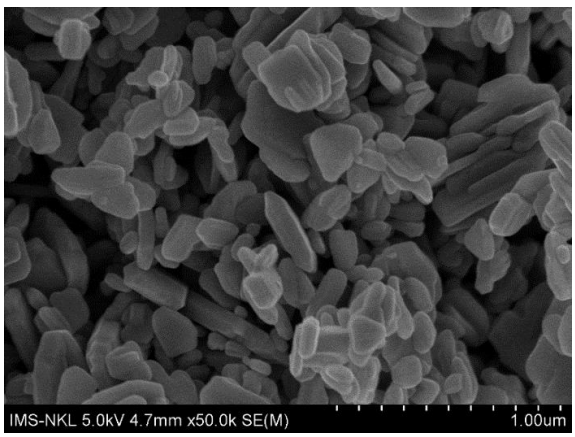

Figure 5. SEM images of Mn-doped (1% mol) ZnO nanoparticles.

The material's surface morphology can be seen from the SEM image of Mn-doped ZnO (Figure 5). This shows that Mn – ZnO materials are short rod-shaped particles with a slightly uniform arrangement, width size of about 19 nm to 56 nm, and length size of about 127 nm to 219 nm.

The synthetic Mn-doped ZnO material is of high purity. This result is proved by the EDS

https://doi.org/10.52111/qnjs.2023.17303

spectra of Mn-doped ZnO (Figure 6). It shows the presence of elements Zn, O, and Mn in the sample. In addition, the presence of foreign elements was not observed.

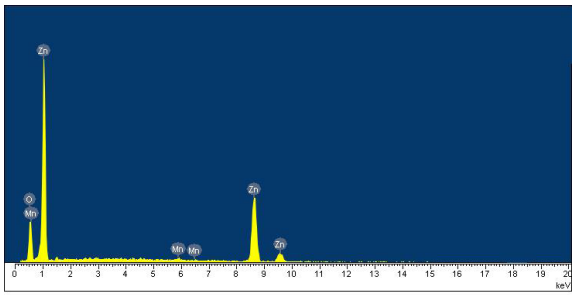

Figure 6. EDS spectra of Mn-doped (1% mol) ZnO nanoparticles.

3.3. Optical activity of metal ion-doped ZnO nanostructures

Photocatalytic activity of representative materials Eu, Mn-doped ZnO was investigated based on MB degradation reaction under UV light. The results of Figure 7 show that the relationship between the optical density and concentration of MB solution has a good linear range at low concentrations. This relationship has relatively good linearity in the MB concentration range from 0.1 to 24 mg/L (correlation coefficient $R^2 = 0.9927$).

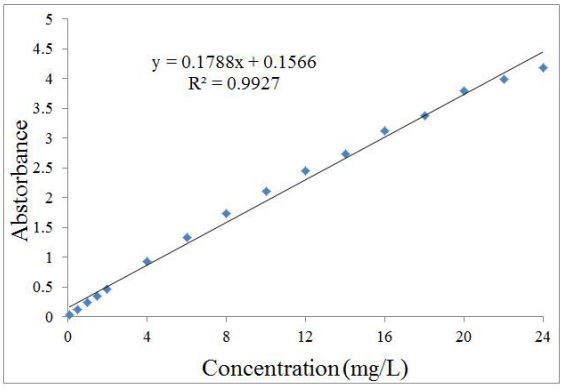

Figure 7. Calibration curve of MB solutions at λ_{max} = 664.4 nm.

However, the best linearity (correlation coefficient $R^2 = 0.9975$) was obtained in the MB concentration range of 4.0 to 16 mg/L. Therefore, the MB concentration of 10 mg/L was chosen for the photocatalytic reaction.

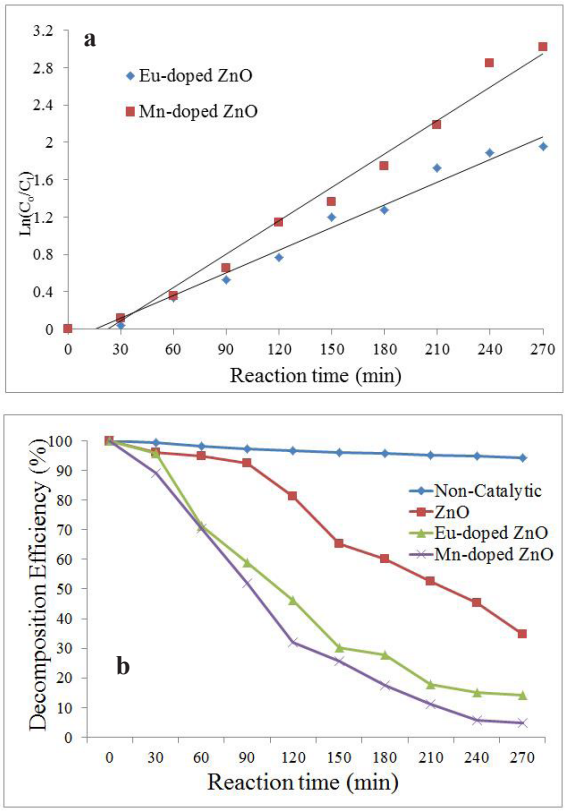

Figure 8. (a) Pseudo first-order rate kinetics for photocatalytic degradation of methylene blue dye; (b) Photodegradation efficiencies of Eu-, Mn-doped ZnO with ZnO.

The lines showing the relationship between $Ln(C_o/C_t)$ and MB decay time were almost linear (Figure 8a). It shows that the MB decomposition reaction kinetics of the materials investigated under the visible light follow the Langmuir – Hinshelwood model and simple 1st-order reaction kinetics. k - the reaction rate constant for Eu-doped ZnO material is 0.008 min^{-1}, and for Mn-doped ZnO material is 0.012 min^{-1}. The reaction rate constant of the Mn-doped ZnO catalyst is higher, which is consistent with the MB decomposition rate of the Mn-doped ZnO catalyst faster than the Eu-doped ZnO.

Figure 8b shows that the degradation efficiency of MB under UV light with Eu- and Mn-doped ZnO is higher than that of undoped ZnO. This result confirmed that europium and manganese doping changed the optical properties of ZnO. Thus, the doping of europium or manganese metal into ZnO increases the

photocatalytic activity of ZnO under UV light. Metal doping into ZnO leads to the formation of a new band gap energy state within the ZnO band gap. On the other hand, the doping of europium or manganese into ZnO increases defects. Both the new band gap energy states and lattice defects are intermediate factors that induce the excitation of electrons from the valence band to the gravitational zone when absorbing visible light.[32] One of the noteworthy effects of manganese doping into ZnO was the increase in defect concentration.[32,33]

3.4. Material reusability

Reusability is one of the essential factors when deciding on a material for the purpose of economic efficiency and environmental protection.[25] After the photocatalytic reaction, the Eu- and Mn-doped ZnO materials were rinsed several times with deionized water, dried at 90 °C for 12 hours, and reused to assess the photocatalytic ability at repeated use. The structure and composition of the crystal phase were examined.

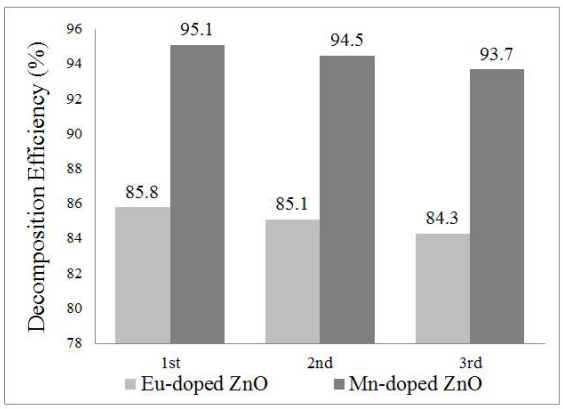

Figure 9. The MB decomposition efficiency of Eu - and Mn-doped ZnO materials after three reuse.

Figure 9 shows the results of the reusability of the two materials Eu- and Mn-doped ZnO. The results show that MB degradation efficiency decreased slightly after each reuse. After reusing them three times, the MB degradation efficiency still reached 84.3% with Eu-doped ZnO and 93.7% with Mn-doped ZnO.

4. CONCLUSION

This study was an attempt to synthesize Eu- and Mn-doped ZnO materials using the hydrothermal method. Data showed high crystallization and photocatalytic activity. In addition, all the materials tested demonstrated reusability. Furthermore, high substrate concentration was shown to inhibit biofilm systems' formation and growth, suggesting that there is an optimal substrate concentration. These findings will provide useful and progressive insights into the future applications of photocatalytic treatment on dye wastes.

REFERENCES

1. A. Boretti, L. Rosa. Reassessing the projections of the world water development report, *NPJ Clean Water,* **2019**, *2*(1), 1-6.
2. K. Vikrant, B. S. Giri, N. Raza, K. Roy, K. H. Kim, B. N. Rai, R. S. Singh. Recent advancements in bioremediation of dye: current status and challenges, *Bioresource Technology,* **2018**, *253*, 355-367.
3. T. Ito, Y. Adachi, Y. Yamanashi, Y. Shimada. Long–term natural remediation process in textile dye–polluted river sediment driven by bacterial community changes, *Water Research,* **2016**, *100*, 458-465.
4. S. Srivastava, R. Sinha, D. Roy. Toxicological effects of malachite green, *Aquatic Toxicology,* **2004**, *66*(3), 319-329.
5. S. Sarmah, A. Kumar. Photocatalytic activity of polyaniline-TiO_2 nanocomposites, *Indian Journal of Physics,* **2011**, *85*(5), 713-726.
6. K. Rao. Inhibition of DNA synthesis in primary rat hepatocyte cultures by malachite green: a new liver tumor promoter, *Toxicology Letters,* **1995**, *81*(2-3), 107-113.
7. D. Alderman, R. C. Hadley. Malachite green: a pharmacokinetic study in rainbow trout, oncorhynchus mykiss (Walbaum), *Journal of Fish Diseases,* **1993**, *16*(4), 297-311.

8. L. Saikia, D. Bhuyan, M. Saikia, B. Malakar, D. K. Dutta, P. Sengupta. Photocatalytic performance of ZnO nanomaterials for self sensitized degradation of malachite green dye under solar light, *Applied Catalysis A: General,* **2015**, *490*, 42-49.

9. M. Qiao, K. Wei, J. Ding, Z. Liu, K. Q. Zhang, X. Huang. Decolorizing activity of malachite green and its mechanisms involved in dye biodegradation by achromobacter xylosoxidans MG1, *Microbial Physiology,* **2011**, *20*(4), 220-227.

10. A. Mittal. Adsorption kinetics of removal of a toxic dye, malachite green, from wastewater by using hen feathers, *Journal of Hazardous Materials,* **2006**, *133*(1-3), 196-202.

11. B. Pare, B. Sarwan, S. Jonnalagadda. Photocatalytic mineralization study of malachite green on the surface of Mn-doped BiOCl activated by visible light under ambient condition, *Applied Surface Science,* **2011**, *258*(1), 247-253.

12. Y. Liu, Y. Ohko, R. Zhang, Y. Yang, Z. Zhang. Degradation of malachite green on Pd/WO_3 photocatalysts under simulated solar light, *Journal of Hazardous Materials,* **2010**, *184* (1-3), 386-391.

13. J. M. Herrmann, J. Disdier, P. Pichat. Effect of chromium doping on the electrical and catalytic properties of powder titania under UV and visible illumination, *Chemical Physics Letters,* **1984**, *108*(6), 618-622.

14. M. M. Khan, S. A. Ansari, D. Pradhan, D. H. Han, J. Lee, M. H. Cho. Defect-induced band gap narrowed CeO_2 nanostructures for visible light activities, *Industrial & Engineering Chemistry Research,* **2014**, *53*(23), 9754-9763.

15. C. Chen, T. Liu, L. Lin, X. Xie, X. Chen, Q. Liu, B. Liang, W. Yu, C. Qiu. Multi-walled carbon nanotube-supported metal-doped ZnO nanoparticles and their photocatalytic property, *Journal of Nanoparticle Research,* **2013**, *15*(1), 1-9.

16. S. Shinde, P. Shinde, C. Bhosale, K. Rajpure. Zinc oxide mediated heterogeneous photocatalytic degradation of organic species under solar radiation, *Journal of Photochemistry and Photobiology B: Biology,* **2011**, *104*(3), 425-433.

17. L. Li, T. Zhai, Y. Bando, D. Golberg. Recent progress of one-dimensional ZnO nanostructured solar cells, *Nano Energy,* **2012**, *1*(1), 91-106.

18. H. Zhang, B. Chen, H. Jiang, C. Wang, H. Wang, X. Wang. A strategy for ZnO nanorod mediated multi-mode cancer treatment, *Biomaterials,* **2011**, *32*(7), 1906-1914.

19. G. Wu, Y. Zhuang, Z. Lin, X. Yuan, T. Xie, L. Zhang. Synthesis and photoluminescence of Dy-doped ZnO nanowires, *Physica E: Low-Dimensional Systems and Nanostructures,* **2006**, *31*(1), 5-8.

20. H. Liu, X. Cheng, H. Liu, J. Yang, Y. Liu, X. Liu, M. Gao, M. Wei, X. Zhang, Y. Jiang. Structural, optical and magnetic properties of Cu and V co-doped ZnO nanoparticles, *Physica E: Low-dimensional Systems and Nanostructures,* **2013**, *47*, 1-5.

21. J. Li, N. Wu. Semiconductor-based photocatalysts and photoelectrochemical cells for solar fuel generation: a review, *Catalysis Science & Technology,* **2015**, *5*(3), 1360-1384.

22. Z. Wang, Y. Liu, B. Huang, Y. Dai, Z. Lou, G. Wang, X. Zhang, X. Qin. Progress on extending the light absorption spectra of photocatalysts, *Physical Chemistry Chemical Physics,* **2014**, *16*(7), 2758-2774.

23. J. I. Langford, A. Wilson. Scherrer after sixty years: a survey and some new results in the determination of crystallite size, *Journal of Applied Crystallography,* **1978**, *11*(2), 102-113.

24. R. Velmurugan, M. Swaminathan. An efficient nanostructured ZnO for dye sensitized degradation of reactive red 120 dye under solar light, *Solar Energy Materials and Solar Cells,* **2011**, *95*(3), 942-950.

25. F. Achouri, S. Corbel, L. Balan, K. Mozet, E. Girot, G. Medjahdi, M. B. Said, A. Ghrabi, R. Schneider. Porous Mn-doped ZnO nanoparticles for enhanced solar and visible light photocatalysis, *Materials & Design,* **2016**, *101*, 309-316.

26. R. Mohammed, M. E. M. Ali, E. Gomaa, M. Mohsen. Green ZnO nanorod material for dye degradation and detoxification of pharmaceutical wastes in water, *Journal of Environmental Chemical Engineering,* **2020**, *8*(5), 104295.

27. T. Ghrib, A. L. A. Otaibi, I. Massoudi, A. M. Alsagry, A. S. Aljaber, E. A. Alhussain, W. S. Alrubian, S. Brini, M. A. Gondal, K. A. Elsayed. Effect of europium doping on the microstructural, optical and photocatalytic properties of ZnO nanopowders, *Arab Journal of Basic and Applied Sciences,* **2022**, *29*(1), 138-149.

28. M. Wang, C. Huang, Z. Huang, W. Guo, J. Huang, H. He, H. Wang, Y. Cao, Q. Liu, J. Liang. Synthesis and photoluminescence of Eu-doped ZnO microrods prepared by hydrothermal method, *Optical Materials,* **2009**, *31*(10), 1502-1505.

29. H. Shahroosvand, M. Ghorbani-asl. Solution-based synthetic strategies for Eu doped ZnO nanoparticle with enhanced red photoluminescence, *Journal of Luminescence,* **2013**, *144*, 223-229.

30. J. E. Ghoul, C. Barthou, M. Saadoun, L. E. Mir. Synthesis and optical characterization of SiO_2/Zn_2SiO_4: Mn nanocomposite, *Physica B: Condensed Matter,* **2010**, *405*(2), 597-601.

31. Y. M. Hao, S. Y. Lou, S. M. Zhou, R. J. Yuan, G. Y. Zhu, N. Li. Structural, optical, and magnetic studies of manganese-doped zinc oxide hierarchical microspheres by self-assembly of nanoparticles, *Nanoscale Research Letters,* **2012**, *7*(1), 1-9.

32. M. A. Mahmood, S. Baruah, J. Dutta. Enhanced visible light photocatalysis by manganese doping or rapid crystallization with ZnO nanoparticles, *Materials Chemistry and Physics,* **2011**, *130*(1-2), 531-535.

33. Q. Xiao, L. Ouyang. Photocatalytic photodegradation of xanthate over $Zn_{1-x}Mn_xO$ under visible light irradiation, *Journal of Alloys and Compounds,* **2009**, *479*(1-2), L4-L7.

https://doi.org/10.52111/qnjs.2023.17303